

Contents lists available at ScienceDirect

Bioorganic & Medicinal Chemistry Letters

journal homepage: http://ees.elsevier.com



Propargylglycine-based antimicrobial compounds are targets of TolC-dependent efflux systems in *Escherichia coli*

Rebeca J. Roldan^a, Andrea O. Pajarillo^a, Jacob D. Greenberg^a, Joyce E. Karlinsey^b, Mauricio Cafiero^a, Elaine R. Frawley^c, Larryn W. Peterson^a,

- ^a Department of Chemistry, Rhodes College, Memphis, TN 38112, USA
- ^b Department of Microbiology, University of Washington, Seattle, WA 98195, USA
- ^c Department of Biology, Rhodes College, Memphis, TN 38112, USA

ARTICLE INFO

Keywords L-Propargylglycine Lipopolysaccharide TolC Antimicrobial Efflux pumps

ABSTRACT

A library of novel L-propargylglycine-based compounds were designed and synthesized with the goal of inhibiting the growth of Gram-negative bacteria by targeting LpxC, a highly conserved Gram-negative enzyme which performs an essential step in the lipid A biosynthetic pathway. These compounds were designed with and without a nucleoside and had varying tail structures, which modulate their lipophilicity. The synthetic scheme was improved compared to previous methods: a methyl ester intermediate was converted to a hydroxamic acid, which obviated the need for a THP protecting group and improved the yields and purity of the final compounds. Antimicrobial activity was observed for non-nucleoside compounds containing a phenyl propargyl ether tail (5) or a biphenyl tail (6). An MIC of $16~\mu g/mL$ was achieved for 6 in *Escherichia coli*, but inhibition was only possible in the absence of TolC-mediated efflux. Compound 5 had an initial MIC $>160~\mu g/mL$ in *E. coli*. Enhancing outer membrane permeability or eliminating efflux reduced the MIC modestly to $100~\mu g/mL$ and $80~\mu g/mL$, respectively. These results highlight the importance of hydrophobicity of this class of compounds in developing LpxC inhibitors, as well as the design challenge of avoiding multidrug efflux activity.

Incidences of multidrug-resistant pathogens have increased on a global basis, with some bacterial strains now exhibiting resistance to even last-resort antibiotics.¹⁻⁹ In the US alone, at nearly 3 million cases of multidrug resistant bacterial infections occur each year, resulting in approximately 35,000 deaths per annum.¹⁰ Development of new antimicrobials that are not subject to existing mechanisms of resistance is an important goal of current research.

Lipopolysaccharides (LPS) are an important structural component of the Gram-negative outer membrane, creating both a physical and charge barrier to permeability by a wide variety of compounds and antibiotics. ^{11–15} Each LPS molecule consists of three sections: an O-antigen, a core oligosaccharide, and a lipid A anchor embedded in the membrane. UDP-(3-O-((R)-3-hydroxymyristoyl))-N-acetylglucosamine deacetylase, or LpxC, is responsible for the first committed step of lipid A synthesis and is essential in *Escherichia coli*. ^{16–18} Inhibition of LpxC prevents LPS formation and enhances antibiotic sensitivity. ^{19–21} LpxC is conserved across Gram-negative phyla and shares no homology with mammalian enzymes, making it an attractive target for antimicrobial treatment. ^{22–24}

Our analysis of the crystal structure of the *Aquifex aeolicus* LpxC active site²⁵ found three target areas for ligand binding: a $\rm Zn^{2+}$ ion, a polar region, and a hydrophobic passage (Fig. 1).^{26,27} The LpxC natural substrate consists of a nucleoside, a diphosphate group, a glucosamine, and a long hydrocarbon tail. The strongest potential interactions can occur with the $\rm Zn^{2+}$ ion via ionic binding.²⁸ Among the LpxC inhibitors found in literature, all share a hydroxamate head group (replacing the diphosphate group of the natural substrate), which binds strongly to the $\rm Zn^{2+}$ ion²⁹ forming a thermodynamically favorable five-membered ring.³⁰ Most inhibitor design has focused on optimizing the tail moiety, and few inhibitors include the nucleoside for binding in the polar region.^{31,32} In this work, potential inhibitors of LpxC capable of targeting two or more regions in the LpxC active site were designed. The structures differ in inclusion of a nucleoside and in type of hydrophobic tail (Fig. 2).

Efficacy of antimicrobial compounds depends not only on their ability to bind and inhibit a specific molecular target, but also to accumulate within bacterial cells. Sufficiently lipophilic compounds can diffuse across the outer and inner membranes, while other compounds enter

E-mail addresses: frawleye@rhodes.edu (E.R. Frawley); petersonl@rhodes.edu (L.W. Peterson)

^{*} Corresponding author.

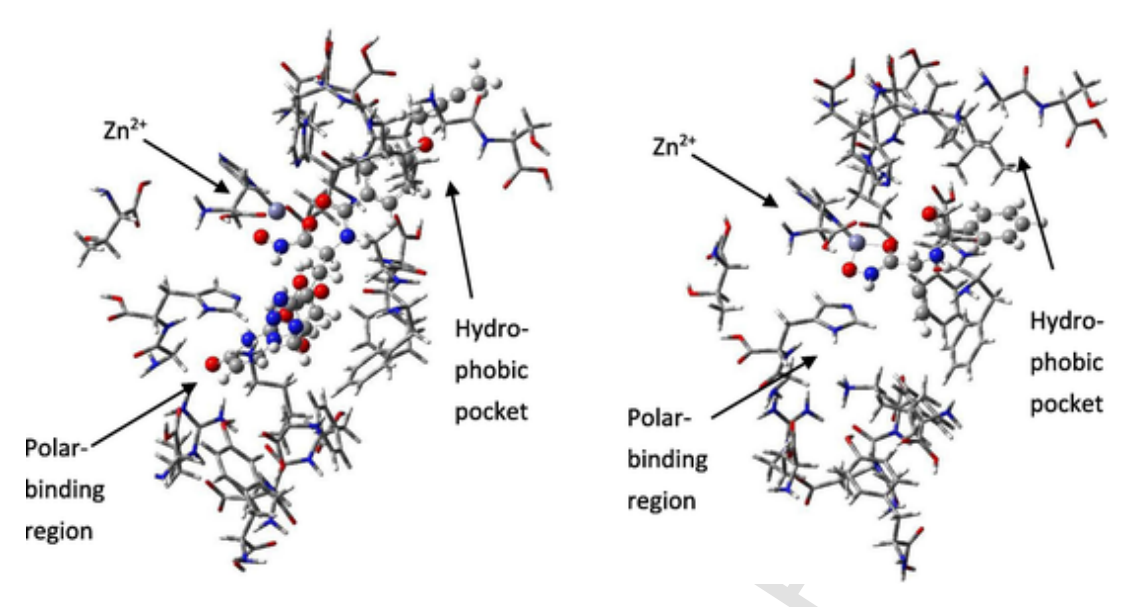
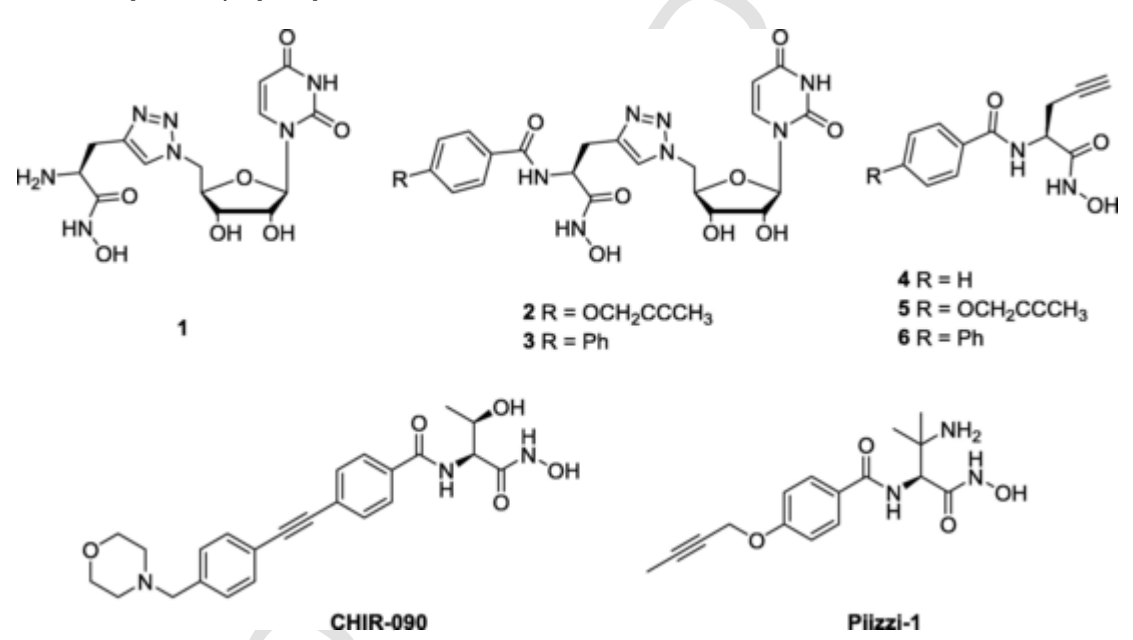


Fig. 1. (Left) Compound **2** (ball and stick) optimized in the *A. aeolicus* LpxC active site (M062X/6-31G) showing the molecule interacting with the binding site via the polar binding region, the Zn²⁺ ion, and the hydrophobic pocket. (Right) Compound **4** (ball and stick) optimized in the *A. aeolicus* LpxC active site (M062X/6-31G) showing the molecule interacting with the binding site via the Zn²⁺ ion, and part of the hydrophobic pocket.²⁷



 $Fig.\ 2.\ The\ structures\ of\ the\ propargylglycine-based\ compounds\ 1-6,\ CHIR-090\ and\ Piizzi-1.$

bacterial cells via channels and porins that are selective according to size and other properties such as hydrophilicity or charge.^{33,34} Once inside the cell, many antimicrobial compounds are the target of various efflux systems including those from the resistance-nodulation-division (RND), major facilitator (MF), ATP-binding cassette (ABC), small multidrug resistance (SMR) and multidrug and toxic compound extrusion (MATE) families. Of these groups, the RND family transporters have the widest range of substrates and account for the majority of intrinsic resistance in Gram-negative bacteria.¹⁵ It remains challenging to predict whether a compound will be targeted for efflux by RND transporters but transport does correlate positively with hydrophobicity.^{15,35}

Herein, we report the synthesis of a new nucleoside-containing compound 2 and the design and synthesis of novel propargylglycine-based compounds designed to inhibit LpxC activity (4–6, Fig. 2). Additionally, a new synthetic procedure, which obviated the need for the THP-protecting group, was implemented to reduce the number of steps and

improve the yield of the final hydroxamic acids. Finally, the minimal inhibitory concentrations (MICs) for compounds **1–6** were established for *P. aeruginosa* and *E. coli*. Improved antibacterial activity was observed in *E. coli* strains with either increased permeability or lacking TolC-dependent efflux.

Being informed by our previous computational work,²⁶ we focus here on synthesizing and testing antimicrobial activity of promising compounds. Compound 1, which does not contain a hydrophobic tail, had the most negative interaction energy at –710 kcal/mol in a solvated model.²⁶ However, as many key human enzymes, such as matrix metalloproteinases and zinc-dependent histone deacetylases, contain Zn²⁺ ions in their active sites, the inclusion of the hydrophobic tail should provide greater specificity for LpxC.

Incorporation of a hydrophobic tail to bind in the active site offers both design and synthetic challenges. The amino acid sequence in these tunnels differs across many Gram-negative strains, resulting in varying passage shape. ³⁶ In order to achieve broad spectrum activity against different Gram-negative species, the tail must be able to fit within a variety of hydrophobic passages and resolve any differences. Many research groups have found that more linear tails can account for slight variations in the hydrophobic tunnel, resulting in a wide variety of tails with aromatic groups bound by acetylene or diacetylene. ³⁷ However, many inhibitors including CHIR-090 (Fig. 2) showed low aqueous solubility as well as *in vitro* cytotoxicity. ³⁷ In place of the diacetylene and acetylene tails, a flexible propargyl ether group was added which could specifically inhibit *P. aeruginosa* LpxC. ³⁸ Piizzi-1 (Fig. 2), with a propargyl ether tail, showed an IC₅₀ value of 0.004 μ M against wild-type *P. aeruginosa* LpxC and MIC₉₀ of 2 μ g/mL in multidrug resistant (MDR) *P. aeruginosa*, as well as good aqueous solubility with no cytotoxic effects. ³⁸ Due to this success, the propargyl ether tail was incorporated into our inhibitors.

The incorporation of a tail moiety allows for further modulation of the lipophilicity and solubility of the compounds, which can be observed in the calculated log P values (Table 1), giving a relative idea of the hydrophobicity of the compounds. The log P and ClogP of CHIR-090 and Piizzi-1 were also determined as a comparison. Compound 1, which does not contain a hydrophobic tail, has the most negative log P value. The other nucleoside-containing compounds (2 and 3) are still fairly hydrophilic, despite compound 3 containing the biphenyl tail group. Although the nucleoside provides additional points for interaction in the active site, the polarity of the nucleoside decreases the relative lipophilicity, possibly providing challenges for getting into the cell and also potentially having a larger desolvation penalty when binding in the active site. Therefore, we decided to also investigate compounds that lack the nucleoside. Compounds 4–6, with just the propar-

Table 1LogP and CLogP values ¹ of synthesized compounds.

Piizzi-1 0.44 0.651 CHIR-090 1.40 1.412 1 -3.52 -5.683	
1 2.52 5.602	
1 -3.52 -5.683	
2 -1.69 -2.921	
3 -0.01 -2.183	
4 0.61 -0.227	
5 1.29 0.923	
6 2.28 1.661	

 $^{^{1}\,}$ Values taken from ChemDraw Professional 18.2.

gylglycine scaffold and various tails, have higher log P values and are more lipophilic.

Compound **6** was initially prepared using an intermediate in the synthesis of compound **3**. Commercially available Fmoc-L-propargylglycine was converted from a carboxylic acid to a tetrahydropyran (THP)-protected hydroxamic acid in the presence of N,N'-dicyclohexylcarbodimide (DCC) coupling agent to afford the alkyne **7** in a 78% yield.²⁶ The Fmoc group was then removed using piperidine and biphenyl carboxylic acid was immediately coupled using DCC to afford **8** in a 68% yield (Scheme 1). Final deprotection of the THP-protected hydroxamic acid **8** was accomplished using *p*-toluenesulfonic acid³⁹ to yield the final product **6** in a 72% yield (Scheme 1). However, due to difficulty in purification resulting from low solubility of **6**, this last step underwent several attempts at optimization, but did not give improved results.

Up until this point, we had routinely used a THP-protecting group after converting the carboxylic acid to a protected hydroxamic acid to result in the alkyne derivative. ²⁶ However, the removal of the THP-protection and purification has proven problematic, and therefore, a new synthetic scheme was created with the aim of affording the coupled product in higher yields. An approach involving converting the carboxylic acid first to a methyl ester and then converting to the hydroxamic acid in the last step of synthesis was attempted. ^{38,40} In the interest of pursuing this method, Fmoc-L-propargylglycine was esterified using thionyl chloride in methanol ⁴¹ to form methyl ester 9 in a 100% yield (Scheme 2). A similar method was also employed with Boc-L-propargylglycine to afford 10 in a 94% yield. Although the Boc group was not observed in the ¹H and ¹³C after esterification, HCl in dioxane was added to ensure the hydrochloride salt was available for coupling.

Compound 10 was coupled with benzoyl chloride to give alkyne 13 in an 86% yield (Scheme 2), which was significantly better than the yield obtained with the Fmoc deprotection and 1-ethyl-3-(3-dimethylaminopropyl)carbodiimide (EDC)/DCC coupling previously employed. The propargyl ether benzoic acid derivative 12 was synthesized as previously described by Piizzi and coworkers. BEDC and HATU (1-[bis(dimethylamino)methylene]-1H-1,2,3-triazolo[4,5-b]pyridinium 3-oxid hexafluorophosphate) were explored to synthesize alkyne 14 (Scheme 2). Following Fmoc deprotection of methyl ester 9 with piperidine, acid 12 was coupled to afford alkyne 14. The EDC procedure had been previously used by our lab, and successfully produced alkyne 14 in a 57% yield. However, the HATU coupling procedure was even more successful, with alkyne 14 afforded in an 81% yield. The synthesis was carried out this way since 14 was already available, but in the future any new syntheses should start with Boc-L-propargylglycine. The

Scheme 2

biphenyl analogue **15** was also prepared using compound **10**, biphenyl carboxylic acid and EDC coupling to produce **15** in a 62% yield.

The coupled methyl esters 13–15 were easily converted to hydroxamic acids 4–6 through treatment with aqueous hydroxylamine 38 in 85–100% yields (Scheme 2). This method resulted in significantly higher yields and avoided the need for column chromatography purification. The structures of alkynes 4–6 were confirmed through 1 H NMR and 13 C NMR and by HR-MS. The purity was confirmed by HPLC.

Copper-catalyzed azide-alkyne cycloaddition (CuAAC) was used to synthesize triazole-linked compounds 1 and 3 with yields from 57 to 76% as previously described. Similar methods were utilized in the synthesis of 2 (Scheme 3). Synthesis of the azidonucleoside 18 was accomplished as described previously. Azide 18 and alkyne 5 were dissolved in acetonitrile, after which copper powder was added to the reaction flask. Following sonication, the reaction ran for 24 h at 35 °C to afford 19 in 39% yield, which was significantly lower than yields previously obtained with the other nucleoside analogues. This reduced yield may be in part due to the presence of the hydroxamic acid.

After purification by column chromatography, compound 19 was treated with trifluoroacetic acid (TFA) in order to remove the ketal protecting group. The final compound was obtained through precipitation from a methanolic solution with diethyl ether. Compound 2 was iso-

lated in a 81% yield, which was slightly better than literature yields of 65–70% for compounds 1 and 3 (Scheme 3). 26 Synthesis of 2 was confirmed with 1 H NMR and 13 C NMR and HR-MS. The purity was confirmed by HPLC.

Purified compounds were dissolved in DMSO and the standard microbroth dilution method was used to determine the minimal inhibitory concentration (MIC) for each compound in the Gram-negative bacteria *Escherichia coli* and *Pseudomonas aeruginosa*.⁴² The results, which were consistent across four independent trials, are summarized in Table 2. Compounds 1–4 failed to show any growth inhibition for either *P. aeruginosa* or *E. coli* compared to the 1% DMSO control (Supplementary Figs. 1 and 2A). Failure to inhibit growth could result from lack of activity against the intended target, but it could also be due to a low cell permeability or intrinsic resistance via multidrug efflux systems. To investigate these possibilities, three *E. coli* strains were generated.

A hyperpermeable strain was constructed by creating plasmid pE-F107 to constitutively express a modified version of the FhuA outer membrane porin ($\Delta C \Delta 4 L FhuA$) that was previously shown to enhance sensitivity to antibiotics that otherwise exhibit low rates of permeability.⁴³ This constitutive expression plasmid does not require antibiotic selection for stable maintenance, thus eliminating the concern that presence of either an inducer or a second antimicrobial compound will

Scheme 3

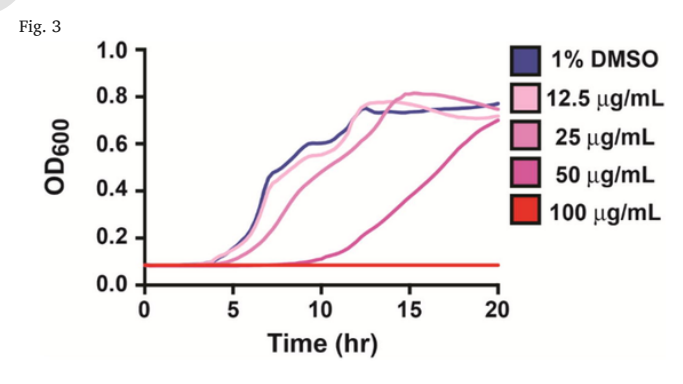
Table 2 MICs for compounds 1–6.

Compound	P. aeruginosa	E. coli	E. coli ΔCΔ4LFhuA	E. coli ΔacrB	E. coli ΔtolC
1	ND 1	ND	ND	ND	ND
2	ND	ND	ND	ND	ND
3	ND	ND	ND	ND	ND
4	ND	ND	ND	ND	ND
5	100 μg/mL	>160 μg/mL	100 μg/mL	80 μg/mL	80 μg/mL
6	ND	ND	ND	$32~\mu g/mL$	16 μg/mL

 $^{^{1}\,}$ ND indicates than inhibition was not observed and an MIC was not able to be determined.

impact the observed MICs. The $\Delta acrB$ strain lacks function of the AcrAB-TolC multi-drug efflux system, which is responsible for the majority of efflux-based resistance in *E. coli.* 44–47 The $\Delta tolC$ strain lacks the outer membrane protein utilized by resistance-nodulation-cell division (RND) family efflux pumps and therefore eliminates the function of all multidrug efflux systems in this family. 44,48,49 Neither the hyperpermeable strain (Supplementary Fig. 2B) nor the efflux mutants (Supplementary Fig. 2C and 2D) showed any difference in sensitivity to compounds 1–4. Though direct interactions of these compounds with LpxC were not determined, the failure to inhibit bacterial growth suggests that the nucleoside-based structures 1–3 are not effective inhibitors of LpxC as modeling suggested, nor does the small tail structure of compound 4 result in antimicrobial activity despite its increased hydrophobicity relative to compounds 1–3.

For *P. aeruginosa*, the MIC for compound **5** was 100 μ g/mL (Fig. 3). For *E. coli*, compound **5** inhibited bacterial growth but it was not possible to determine an MIC (Fig. 4A). Despite sharing 57.4% sequence identity and 79.7% sequence similarity for LpxC, there are modest differences between the structures of the *P. aeruginosa* and *E. coli* enzymes that could account for this difference.³⁶ It is also possible that differences in outer membrane permeability or efflux activity between these species account for the observed difference. In the *E. coli* strain expressing $\Delta C \Delta 4 L F h u A$, the MIC for compound **5** was $100 \mu g/m L$ (Fig. 4B) while in the $\Delta acr B$ and $\Delta tol C$ efflux mutants, the MIC was modestly reduced to $80 \mu g/m L$ (Fig. 4C and 4D). From these results we conclude that the intermediate hydrophobicity of compound **5** limited its permeability across the *E. coli* outer membrane but was still sufficient for compound that did enter to be targeted by the AcrAB-TolC efflux

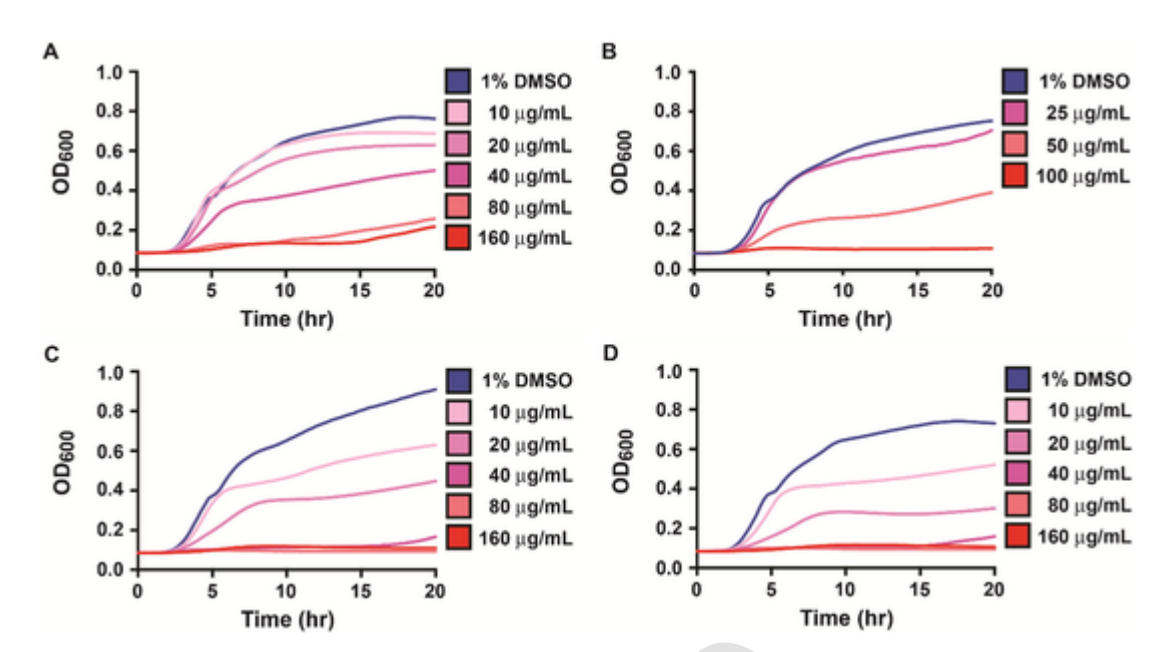


Compound 5 completely inhibits growth of *P. aeruginosa* at 100 μ g/mL. Compound 5 delays growth of *P. aeruginosa* at 25 μ g/mL (pink) and 50 μ g/mL (dark pink) compared to 1% DMSO alone (blue) with complete inhibition at 100 μ g/mL (red).

pump. When permeability was enhanced or efflux eliminated, compound 5 was able to prevent *E. coli* growth.

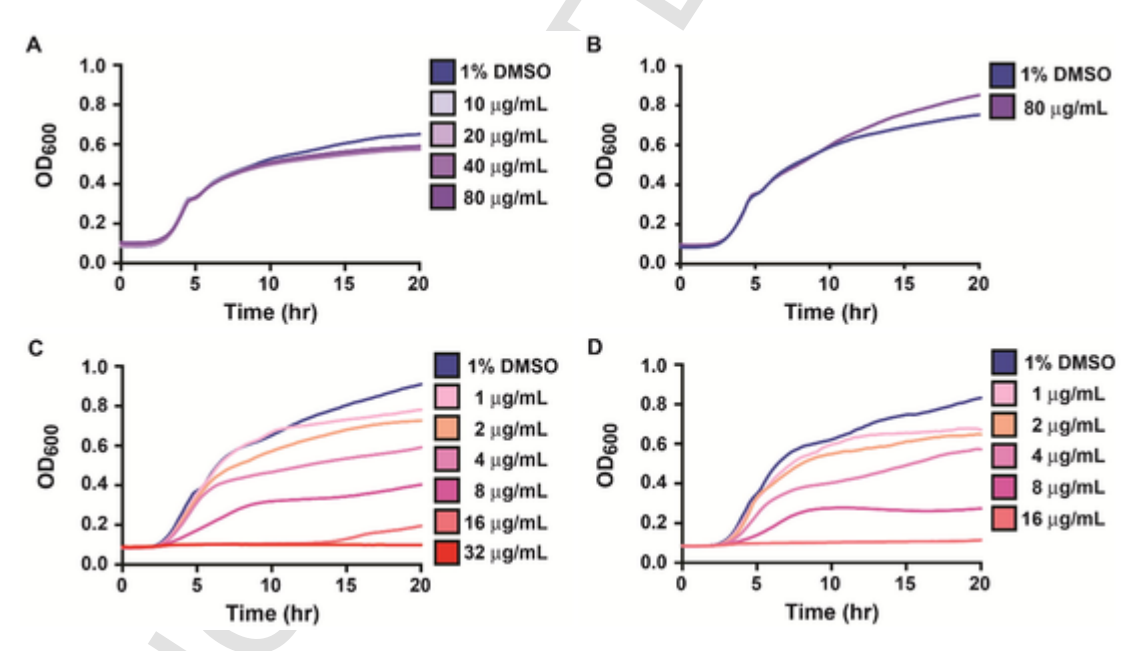
For compound **6**, no MIC could initially be established for either *P. aeruginosa* (Supplementary Fig. 5) or *E. coli* (Fig. 5A). Similarly, no MIC could be determined in the hyperpermeable *E. coli* strain expressing $\Delta C \Delta 4 L F huA$ (Fig. 5B). It was possible to determine an MIC of 32 µg/mL in the $\Delta acrB$ strain (Fig. 5C) and 16 µg/mL in the $\Delta tolC$ strain (Fig. 5D). Expressing $\Delta C \Delta 4 L F huA$ in combination with either the $\Delta acrB$ or $\Delta tolC$ mutation did not further alter the MICs (data not shown). These results demonstrate that compound **6**, the most hydrophobic compound tested, was not limited in its ability to enter *E*.

Fig. 4



Compound 5 completely inhibits growth of *E. coli* when outer membrane permeability is enhanced or multidrug efflux eliminated. A) Compound 5 inhibits growth of *E. coli* in a dose dependent manner compared to 1% DMSO alone (blue) but a minor amount of growth is still observed at 160 μ g/mL (red). B) Expression of the engineered outer membrane porin Δ C Δ 4LFhuA results in complete inhibition of growth by compound 5 at 100 μ g/mL (red). C) The Δ acrB strain which lacks function of the AcrAB-TolC multidrug efflux system is sensitive to compound 5 with complete inhibition of growth occurring at 80 μ g/mL (orange). D) The Δ tolC mutant which lacks function of all RND-family efflux systems is no more sensitive to compound 5 than the Δ acrB strain and also exhibits complete inhibition of growth at 80 μ g/mL (orange). (For interpretation of the references to colour in this figure legend, the reader is referred to the web version of this article.)

Fig. 5



Compound 6 completely inhibits growth of *E. coli* when multidrug efflux is eliminated. A) Compound 6 fails to inhibit growth of *E. coli* compared to 1% DMSO alone (blue), at the solubility limit of 80 μ g/mL (darkest purple). B) Expression of Δ C Δ 4LFhuA does not result in growth inhibition by 80 μ g/mL compound 6 (purple) compared to 1% DMSO (blue). C) A Δ acrB mutant lacking function of the AcrAB-TolC multidrug efflux system is inhibited by compound 6 in a dose-dependent manner compared to 1% DMSO (blue) with complete inhibition at 32 μ g/mL (red). D) A Δ tolC mutant lacking function of all RND-family efflux systems displays increased sensitivity to compound 6 with complete inhibition at 16 μ g/mL. (For interpretation of the references to colour in this figure legend, the reader is referred to the web version of this article.)

coli cells but rather lack of inhibition was due to the activity of multiple drug efflux systems. The AcrAB-TolC multidrug efflux system was responsible for the majority of the intrinsic resistance of *E. coli* to this compound. However, compound 6 was a substrate for other RND-family efflux systems as well since deletion of tolC lead to a further 2-fold decrease in MIC. It is likely that we were unable to observe inhibition of *P. aeruginosa* growth by compound 6 due to similar efflux mecha-

nisms in this organism. Intrinsic antibiotic resistance in P. aeruginosa is mediated primarily by the MexAB-OprM efflux system, which is also an RND-family efflux pump with a broad substrate range though, as in E. coli, multiple efflux systems are present in the genome. $^{50-53}$

It is notable that both compounds 5 and 6 demonstrated some degree of bacterial growth inhibition, while compound 4 did not. While its lower hydrophobicity may have reduced its ability to enter cells, the

relatively small size of this compound should allow it to readily enter the ΔCΔ4LFhuA-expressing strain. Lack of antimicrobial activity by compound 4 in this genetic background suggests that a larger hydrophobic tail may be required to mediate the molecular interaction, presumably with LpxC, that results in growth inhibition. This is corroborated by the modest inhibition seen with the slightly larger tail of 5 and greatest inhibition with the largest and most hydrophobic tail of 6. This effect may also be explained by the entropic contributions to the Gibbs energy of binding. As has been mentioned, the active site has a large polar region as well as a metal-binding region. This suggests that waters bound in this active site before ligand binding are held tightly and a large desolvation energy penalty is paid when the ligands bind, greatly reducing the enthalpic contribution to the Gibbs energy of binding.²⁷ The entropic contribution is thus proportionately more important. When comparing 4 with 5 and 6, we see that the latter two have considerably more degrees of freedom in the hydrophobic tail, and thus more entropy that is lost upon binding (assuming that the hydrophobic tail assumes a somewhat rigid position upon binding). This will be explored further in future computational work.

Unfortunately, the increased hydrophobicity also seems to potentiate efflux. Little structural similarity has been observed among known substrates of RND efflux systems but one common feature appears to be hydrophobicity, with more hydrophobic compounds exhibiting increased efflux. 35,54 Development of AcrAB-TolC inhibitors is an area of significant interest since they would function as adjuvants for a range of antimicrobial compounds but none of these inhibitors has yet entered clinical trials. $^{55-61}$ Future work must focus on developing structures that are effective inhibitors of LpxC without being targeted as substrates for efflux.

Inhibition of bacterial growth by compounds designed to target LpxC activity is a promising method of antibacterial treatment that may be useful against multidrug resistant bacteria. We investigated the use of nucleoside-containing compounds 1-3 designed to mimic the natural substrate of LpxC and interact with the polar region of the binding site, the Zn²⁺ ion and the hydrophobic region (in 2 and 3). Although the nucleoside provides additional points for interaction, based on modeling, it also decreases the log P of the potential inhibitors. Therefore, we sought to increase the lipophilicity of the potential inhibitors and removed the nucleoside and subsequently increased the lipophilicity. Furthermore, the removal of the nucleoside simplifies the synthetic pathway, allowing access to the compounds in higher yields and fewer steps. Compound 2 was synthesized in 7 steps from methyl 4-hydroxybenzoate in a yield of 19%. Compound 4 was fully synthesized in 3 steps with an overall yield of 69%. Compound 5 was fully synthesized in 5 steps with an overall yield of 61%. Compound 6 was synthesized in in 3 steps in an overall 58% yield. Ultimately, the use of a methyl ester instead of the THP-protecting group resulted in higher yields and fewer steps and purifications (58% versus 38% for compound 6).

Nucleoside-containing propargylglycine compounds 1-3 were not effective at inhibiting the growth of E. coli or P. aeruginosa but activity was observed for other propargylglycine compounds. The non-nucleoside compound 4 was also not effective in inhibiting the growth of either E. coli or P. aeruginosa. The most effective activity was displayed by compound 6, which contains a large hydrophobic biphenyl tail, while modest antimicrobial activity was observed for compound 5 containing a phenyl propargyl ether tail. Interestingly, compound 5 and Piizzi-1 (MIC = $2 \mu g/mL$)³⁸ display different MICs for P. aeruginosa despite sharing a common tail structure. They differ in the side chain of the amino acid with compound 5 having an alkyne and Piizzi-1 having a dimethylamino group, which suggests that, while presence of the full nucleoside did not improve activity, presence of a different polar group may. The ArcAB-TolC multidrug efflux system provided significant intrinsic resistance to both of these compounds in E. coli with the greatest efflux-mediated resistance observed for compound 6. The seeming requirement of a large hydrophobic tail for effective growth inhibition therefore presents a significant challenge for future inhibitor design.

Funding

This research did not receive any specific grant from funding agencies in the public, commercial, or not-for-profit sectors.

Declaration of Competing Interest

The authors declare that they have no known competing financial interests or personal relationships that could have appeared to influence the work reported in this paper.

Acknowledgments

High resolution mass spectra were recorded on a Waters Synapt High Resolution Mass Spectrometer housed at the University of Memphis, Department of Chemistry. Prof. Paul Simone and Mr. Drake Williams (University of Memphis) are thanked for assistance with obtaining HRMS data. The authors also thank Prof. Liviu Movileanu and Syracuse University for the gift of pPR-IBA1-FhuA Δ C/ Δ 4L.

Appendix A. Supplementary data

Supplementary data (full synthetic procedures, Figs. S1–S3: growth curves and Figs. S4–S12: 1 H and 13 C NMRs of final compounds **2**, **4**–6) to this article can be found online at https://doi.org/10.1016/j.bmcl.2019. 126875.

References

- MO Ahmed, KE Baptiste. Vancomycin-Resistant Enterococci: A Review of Antimicrobial Resistance Mechanisms and Perspectives of Human and Animal Health. Microbial Drug Resistance; New Rochelle. 2018;24:590–606.
- C-W Chen, H-J Tang, C-C Chen, et al. The Microbiological Characteristics of Carbapenem-Resistant Enterobacteriaceae Carrying the mcr-1 Gene. J Clin Med. 2019;8:(2).
- L Chen. Notes from the Field: Pan-Resistant New Delhi Metallo-Beta-Lactamase-Producing Klebsiella pneumoniae — Washoe County, Nevada, 2016. MMWR Morb Mortal Wkly Rep. 2017;66.
- H Grundmann, C Glasner, B Albiger, et al. Occurrence of carbapenemase-producing Klebsiella pneumoniae and Escherichia coli in the European survey of carbapenemase-producing Enterobacteriaceae (EuSCAPE): a prospective, multinational study. Lancet Infect Dis. 2017;17:153–163.
- AY Guh, SN Bulens, Y Mu, et al. Epidemiology of Carbapenem-Resistant Enterobacteriaceae in 7 US Communities, 2012–2013. JAMA. 2015;314:1479–1487.
- WA McGuinness, N Malachowa, FR DeLeo. Vancomycin Resistance in Staphylococcus aureus. Yale J Biol Med. 2017;90:269–281.
- AAA Sulaiman, II Kassem. First report on the detection of the plasmid-borne colistin resistance gene mcr-1 in multi-drug resistant E. coli isolated from domestic and sewer waters in Syrian refugee camps in Lebanon. Travel Med Infect Dis. 2019.
- Q Wang, X Wang, J Wang, et al. Phenotypic and Genotypic Characterization of Carbapenem-resistant Enterobacteriaceae: Data From a Longitudinal Large-scale CRE Study in China (2012–2016). Clin Infect Dis. 2018;67:S196–S205.
- M Zalipour, BN Esfahani, SA Havaei. Phenotypic and genotypic characterization
 of glycopeptide, aminoglycoside and macrolide resistance among clinical isolates
 of *Enterococcus faecalis*: a multicenter based study. BMC Res Notes. 2019;12.
- CDC Antibiotic resistance threats in the United States, 2019 (accessed December 5, 2019).
- L Leive. The barrier function of the Gram-negative envelope. Ann N Y Acad Sci. 1974;235:109–129.
- H Nikaido. Permeability of the Outer Membrane of Bacteria. Angew Chem, Int Ed Engl. 1979;18:337–350.
- H Nikaido, T Nakae. The outer membrane of Gram-negative bacteria. Adv Microb Physiol. 1979;20:163–250.
 H Nikaido, M Vagra, Molecular basis of bacterial outer membrane permeability.
- H Nikaido, M Vaara. Molecular basis of bacterial outer membrane permeability. Microbiol Rev. 1985;49:1–32.
- X-Z Li, P Plesiat, H Nikaido. The challenge of efflux-mediated antibiotic resistance in Gram-negative bacteria. Clin Microbiol Rev. 2015;28:337–418.
- MS Anderson, HG Bull, SM Galloway, et al. UDP-N-acetylglucosamine acyltransferase of *Escherichia coli*. The first step of endotoxin biosynthesis is thermodynamically unfavorable. J Biol Chem. 1993;268:19858–19865.

- B Beall, J Lutkenhaus. Sequence analysis, transcriptional organization, and insertional mutagenesis of the envA gene of Escherichia coli. J Bacteriol. 1987;169:5408-5415.
- K Young, LL Silver, D Bramhill, et al. The envA permeability/cell division gene of *Escherichia coli* encodes the second enzyme of lipid A biosynthesis. UDP-3-O-(R-3-hydroxymyristoyl)-N-acetylglucosamine deacetylase. J Biol Chem. 1995;270:30384–30391.
- S Normark. Genetics of a chain-forming mutant of *Escherichia coli*. Transduction and dominance of the *envA* gene mediating increased penetration to some antibacterial agents. Genet Res. 1970;16:63–78.
- S Normark, HG Boman, E Matsson. Mutant of Escherichia coli with anomalous cell
 division and ability to decrease episomally and chromosomally mediated resistance to ampicillin and several other antibiotics. J Bacteriol. 1969;97:1334–1342.
- K Young, LL Silver. Leakage of periplasmic enzymes from envA1 strains of Escherichia coli. J Bacteriol. 1991;173:3609–3614.
- HR Onishi, BA Pelak, LS Gerckens, et al. Antibacterial agents that inhibit lipid A biosynthesis. Science (Washington, D.C.). 1996;274:980–982.
- 23. CRH Raetz. Biochemistry of Endotoxins. Annu Rev Biochem. 1990;59:129-170.
- JM Williamson, MS Anderson, CR Raetz. Acyl-acyl carrier protein specificity of UDP-GlcNAc acyltransferases from Gram-negative bacteria: relationship to lipid A structure. J Bacteriol. 1991;173:3591–3596.
- HA Gennadios, DW Christianson. Binding of Uridine 5'-Diphosphate in the "Basic Patch" of the Zinc Deacetylase LpxC and Implications for Substrate Binding. Biochemistry. 2006;45:15216–15223.
- S Malkowski, C Dishuck, G Lamanilao, et al. Design, Modeling and Synthesis of 1,2,3-Triazole-Linked Nucleoside-Amino Acid Conjugates as Potential Antibacterial Agents. Molecules. 2017;22:1682.
- Roldan, RJ, Embry, CP, Peterson, LW, Cafiero, M, Evaluation of DFT and ONIOM
 calculations for the binding of novel ligands in the LpxC enzyme active site, in
 preparation
- AW Barb, P Zhou. Mechanism and inhibition of LpxC: An essential zinc-dependent deacetylase of bacterial lipid a synthesis. Curr Pharm Biotechnol. 2008;9:9–15.
- K Zuo, L Liang, W Du, et al. 3D-QSAR, Molecular Docking and Molecular Dynamics Simulation of *Pseudomonas aeruginosa* LpxC Inhibitors. Int J Mol Sci. 2017;18:(5)
- JC Dewar, AS Thakur, WW Brennessel, M Cafiero, LW Peterson, WT Eckenhoff. Simple zinc complex to model substrate binding to zinc enzymes. Inorg Chim Acta. 2018;473:15–19.
- AW Barb, TM Leavy, LI Robins, et al. Uridine-Based Inhibitors as New Leads for Antibiotics Targeting Escherichia coli LpxC. Biochemistry. 2009;48:3068–3077.
- SK Jana, M Loeppenberg, CG Daniliuc, R Holl. C-Triazolyl β-D-furanosides as LpxC inhibitors: stereoselective synthesis and biological evaluation. Tetrahedron. 2014:70:6569–6577.
- H Nikaido. Molecular basis of bacterial outer membrane permeability revisited. Microbiol Mol Biol Rev. 2003;67:593

 –656.
- AH Delcour. Outer membrane permeability and antibiotic resistance. Biochim Biophys Acta, Proteins Proteomics. 2009;1794:808–816.
- H Nikaido, M Basina, V Nguyen, EY Rosenberg. Multidrug efflux pump AcrAB of Salmonella typhimurium excretes only those beta-lactam antibiotics containing lipophilic side chains. J Bacteriol. 1998;180:4686–4692.
- C-J Lee, X Liang, X Chen, et al. Species-Specific and Inhibitor-Dependent Conformations of LpxC: Implications for Antibiotic Design. Chem Biol. 2011;18:38–47.
- X Liang, C-J Lee, X Chen, et al. Syntheses, structures and antibiotic activities of LpxC inhibitors based on the diacetylene scaffold. Bioorg Med Chem. 2011:19:852–860.
- G Piizzi, DT Parker, Y Peng, et al. Design, Synthesis, and Properties of a Potent Inhibitor of *Pseudomonas aeruginosa* Deacetylase LpxC. J Med Chem. 2017;60:5002–5014.
- F Brandhuber, M Zengerle, L Porwol, et al. Tabun scavengers based on hydroxamic acid containing cyclodextrins. Chem Commun. 2013;49:3425–3427.
- X Liang, R Gopalaswamy, F Navas, EJ Toone, P Zhou. A Scalable Synthesis of the Difluoromethyl-allo-threonyl Hydroxamate-Based LpxC Inhibitor LPC-058. J Org Chem. 2016;81:4393–4398.

- ME Ourailidou, A Lenoci, C Zwergel, D Rotili, A Mai, FJ Dekker. Towards the development of activity-based probes for detection of lysine-specific demethylase-1 activity. Bioorg Med Chem. 2017;25:847–856.
- CLSI. Methods for dilution antimicrobial susceptibility tests for bacteria that grow aerobically; approved standard - tenth edition. Vol. 35. Clinical and Laboratory Standards Institute; 2015.
- G Krishnamoorthy, D Wolloscheck, JW Weeks, C Croft, VV Rybenkov, HI Zgurskaya. Breaking the Permeability Barrier of *Escherichia coli* by Controlled Hyperporination of the Outer Membrane. Antimicrob Agents Chemother. 2016;60:7372–7381.
- JA Fralick. Evidence that TolC is required for functioning of the Mar/AcrAB efflux pump of Escherichia coli. J Bacteriol. 1996;178:5803–5805.
- H Nikaido, HI Zgurskaya. AcrAB and related multidrug efflux pumps of Escherichia coli. J Mol Microbiol Biotechnol. 2001;3:215–218.
- H Okusu, D Ma, H Nikaido. AcrAB efflux pump plays a major role in the antibiotic resistance phenotype of *Escherichia coli* multiple-antibiotic-resistance (Mar) mutants. J Bacteriol. 1996;178:306–308.
- MC Sulavik, C Houseweart, C Cramer, et al. Antibiotic susceptibility profiles of Escherichia coli strains lacking multidrug efflux pump genes. Antimicrob Agents Chemother. 2001;45:1126–1136.
- T Horiyama, A Yamaguchi, K Nishino. TolC dependency of multidrug efflux systems in Salmonella enterica serovar Typhimurium. J Antimicrob Chemother. 2010;65:1372–1376.
- K Nishino, J Yamada, H Hirakawa, T Hirata, A Yamaguchi. Roles of TolC-dependent multidrug transporters of *Escherichia coli* in resistance to beta-lactams. Antimicrob Agents Chemother. 2003;47:3030–3033.
- XZ Li, H Nikaido, K Poole. Role of mexA-mexB-oprM in antibiotic efflux in Pseudomonas aeruginosa. Antimicrob Agents Chemother. 1995;39:1948–1953.
- 51. Y Morita, Y Komori, T Mima, T Kuroda, T Mizushima, T Tsuchiya. Construction of a series of mutants lacking all of the four major mex operons for multidrug efflux pumps or possessing each one of the operons from Pseudomonas aeruginosa PAO1: MexCD-OprJ is an inducible pump. FEMS Microbiol Lett. 2001;202:139–143.
- T Nakae, A Nakajima, T Ono, K Saito, H Yoneyama. Resistance to beta-lactam antibiotics in *Pseudomonas aeruginosa* due to interplay between the MexAB-OprM efflux pump and beta-lactamase. Antimicrob Agents Chemother. 1999;43:1301–1303.
- K Poole, K Krebes, C McNally, S Neshat. Multiple antibiotic resistance in Pseudomonas aeruginosa: evidence for involvement of an efflux operon. J Bacteriol. 1993;175:7363–7372.
- H Nikaido. Multidrug efflux pumps of Gram-negative bacteria. J Bacteriol. 1996:178:5853–5859.
- 55. JA Bohnert, S Schuster, WV Kern, et al. Novel Piperazine Arylideneimidazolones Inhibit the AcrAB-TolC Pump in Escherichia coli and Simultaneously Act as Fluorescent Membrane Probes in a Combined Real-Time Influx and Efflux Assay. Antimicrob Agents Chemother. 2016;60:1974–1983.
- A Kincses, A Szabó, R Saijo, et al. Fluorinated Beta-diketo Phosphorus Ylides Are Novel Efflux Pump Inhibitors in Bacteria. Vivo. 2016;30:813–817.
- ST Nguyen, SM Kwasny, X Ding, et al. Structure-Activity Relationships of a Novel Pyranopyridine Series of Gram-negative Bacterial Efflux Pump Inhibitors. Bioorg Med Chem. 2015;23:2024–2034.
- TJ Opperman, SM Kwasny, H-S Kim, et al. Characterization of a Novel Pyranopyridine Inhibitor of the AcrAB Efflux Pump of Escherichia coli. Antimicrob Agents Chemother. 2014;58:722–733.
- H Sjuts, AV Vargiu, SM Kwasny, et al. Molecular basis for inhibition of AcrB multidrug efflux pump by novel and powerful pyranopyridine derivatives. Proc Natl Acad Sci USA. 2016;113:3509–3514.
- AV Vargiu, P Ruggerone, TJ Opperman, ST Nguyen, H Nikaido. Molecular Mechanism of MBX2319 Inhibition of Escherichia coli AcrB Multidrug Efflux Pump and Comparison with Other Inhibitors. Antimicrob Agents Chemother. 2014;58:6224–6234.
- S Yilmaz, G Altinkanat-Gelmez, K Bolelli, et al. Binding site feature description of 2-substituted benzothiazoles as potential AcrAB-TolC efflux pump inhibitors in E. coli. SAR QSAR Environ Res. 2015;26:853–871.